

MaTe3D: Mask-guided Text-based 3D-aware Portrait Editing

Kangneng Zhou^{1,*} Daiheng Gao² Xuan Wang^{3,✉} Jie Zhang^{4,5,6} Peng Zhang²
 Xusen Sun⁷ Longhao Zhang² Shiqi Yang⁸ Bang Zhang² Liefeng Bo² Yaxing Wang^{1,✉}

¹VCIP,CS, Nankai University, ²Institute for Intelligent Computing, Alibaba Group,

³Ant Group, ⁴School of Design, The Hong Kong Polytechnic University,

⁵Faculty of Innovation and Design, City University of Macau,

⁶Department of Computing, The Hong Kong Polytechnic University,

⁷Nanjing University, ⁸Computer Vision Center, Universitat Autònoma

elliszkn@163.com {daiheng.gdh, funtian.zp, longhao.zlh, zhangbang.zb, liefeng.bo}@alibaba-inc.com

xwang.cv@gmail.com peterzhang1130@163.com xusensun@smail.nju.edu.cn

syang@cvc.uab.es yaxing@nankai.edu.cn

<https://humanaigc.github.io/MaTe3D/>

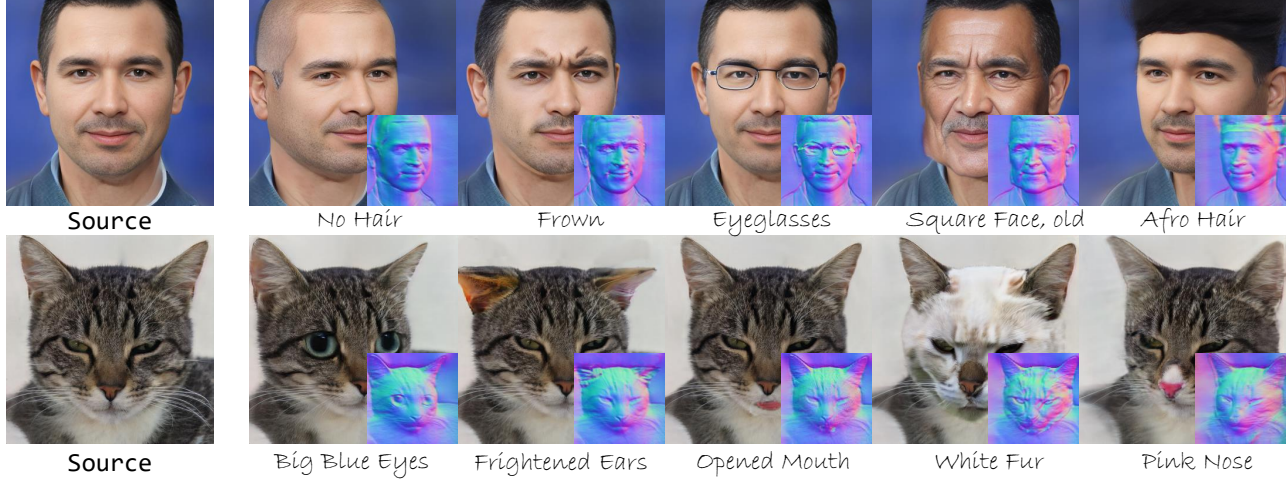


Figure 1. Mask-guided Text-based portrait editing. Given a image, MaTe3D is able to learn a photorealistic 3D radiance field using a text prompt and a target mask. It synthesizes stable and finely detailed texture while ensuring consistency between texture and geometry.

Abstract

Recently, 3D-aware face editing has witnessed remarkable progress. Although current approaches successfully perform mask-guided or text-based editing, these properties have not been combined into a single method. To address this limitation, we propose **MaTe3D**: mask-guided text-based 3D-aware portrait editing. First, we propose a new SDF-based 3D generator. To better perform masked-based editing (mainly happening in local areas), we propose SDF and density consistency losses, aiming to effectively model both the global and local representations jointly. Second,

we introduce an inference-optimized method. We introduce two techniques based on the SDS (Score Distillation Sampling), including a blending SDS and a conditional SDS. The former aims to overcome the mismatch problem between geometry and appearance, ultimately harming fidelity. The conditional SDS contributes to further producing satisfactory and stable results. Additionally, we create CatMask-HQ dataset, a large-scale high-resolution cat face annotations. We perform experiments on both the FFHQ and CatMask-HQ datasets to demonstrate the effectiveness of the proposed method. Our method generates faithfully a edited 3D-aware face image given a modified mask and a text prompt. Our code and models will be publicly released.

* Work done as an intern at Alibaba Group.

1. Introduction

Benefiting from StyleGAN-series [15–17], EG3D [4] and its concurrent works [9, 27, 45] have successfully generated high-quality view-consistent, detailed 3D scenes by combining NeRF [23] with the adversarial mechanism [8]. Furthermore, this recent progress [14, 39, 40] in 3D-aware image synthesis investigates the view-consistent image editability conditioning additional information, where the aim to meet diverse users’ needs.

Existing NeRF-based generation methods with editability could be briefly divided into two classes: *mask-guided* [39, 40] and *text-guided* [14, 41]. Mask-guided method aims to support user-friendly editing via hand-drawing sketch or semantic label interface. IDE-3D [39] achieves high-quality and real-time local face control via manipulating the semantic map. However, the existing mask-guided methods mainly focus on shape control, and fail to perform texture control. Text-guided methods aim to generate more expressive results corresponding to textual descriptions via distilling the prior knowledge from large models, e.g., CLIP [30] and diffusion model [33]. LENeRF [14] leverages CLIP [30] to achieve fine-grained and localized manipulation with text inputs. However, existing text-based methods struggle to accurately control shape and produce desired results.

The utilization of both the mask and the text leads to numerous advantages, such as disentangling structure and texture, diverse local editing. To achieve these properties, a straightforward strategy is to merge mask-guided and text-guided techniques presented in the aforementioned part. However, we found that simply equipping previous SOTAs with additional branches failed to balance mask and text effectively. This conflict leads the results towards mask or text, rather than achieving a optimal point consistent with both, as shown in Fig. 6.

Unfortunately, there are no prior tailored works investigating how to integrate effectively both mask-guided and text-guided manipulation in a single model without conflict. To address this limitation, we propose *MaTe3D*. To achieve these properties, we decouple MaTe3D into two steps. First, we learn a new SDF-based 3D generator. Different from prior works (e.g., StyleSDF [27]) only learning the global representation, we also explicitly study the local representations. Since performing mask-guided editing mainly happens in local areas, explicitly modeling the local representations contributes to conducting mask-guided editing. However, optimizing such a generator is hard with the aim to learn simultaneously the global and local representations. Thus, we propose two new objectives: SDF and density consistency losses. These techniques contribute to effectively integrating global and local representations. Additionally, the extra benefit of an SDF-based 3D generator is that we are able to directly derive semantic probability,

which helps to achieve well-established geometry and view-consistency editing results (Fig. 4 and Fig. 7).

Second, we introduce an inference-optimized editing method. When directly manipulating the generator with both mask and text information, the system suffers from two challenges: *3D quality degradation* and *unstable appearance*, see Fig. 8. To overcome these limitations, we introduce two techniques based on the Score Distillation Sampling (SDS) [29], including a blending SDS loss and a conditional SDS loss. The former aims to overcome the mismatch problem between texture and geometry, which leads to 3D quality degradation. We compute SDS considering the dynamic blend of image and normal. The conditional SDS loss improves insufficient 3D-aware control, avoiding an unstable appearance. The original SDS loss [29] directly computes the gradient and updates a generator. However, we find it fails to obtain fine-grained and localized manipulation. Therefore, we train a ControlNet conditioning both semantic mask and RGB. In our inference-optimized editing stage, we frozen the well-trained ControlNet, and update the generator with our blending and conditional SDS losses. Further, since the 3D-aware target mask annotation is lacking, we propose to calculate conditional SDS loss with the mask rendered from the generator. This strategy remedies the multi-view ambiguity in diffusion model and enhances texture stability effectively. To support extensive studies on our proposed method, we created CatMask-HQ annotations, which are large-scale high-resolution cat face annotations specifically designed for the AFHQ dataset. To summarize, we make the following contributions:

- We propose a compact and effective framework: MaTe3D, that performs mask-guided and text-based portrait editing in a single model. Note that current models only possess one of these desirable properties, whereas our model achieves both simultaneously.
- We decouple MaTe3D into two steps. First, we propose a new SDF-based 3D generator. To train this SDF-based 3D generator effectively, we provide several techniques: hierarchical (i.e., local and global) representation learning, SDF and density consistency losses. The second step is the proposal of new editing losses: blending SDS and conditional SDS.
- We create a cat face annotation dataset called CatMask-HQ to support extensive experiments with our method.
- We conduct extensive qualitative and quantitative experiments. The results show that our method is able to perform mask-guided and text-based portrait editing simultaneously.

2. Related Works

3D-aware GANs. Shocked by NeRF [23] and SIREN [37] in exceeding the past method in view of multi-view im-

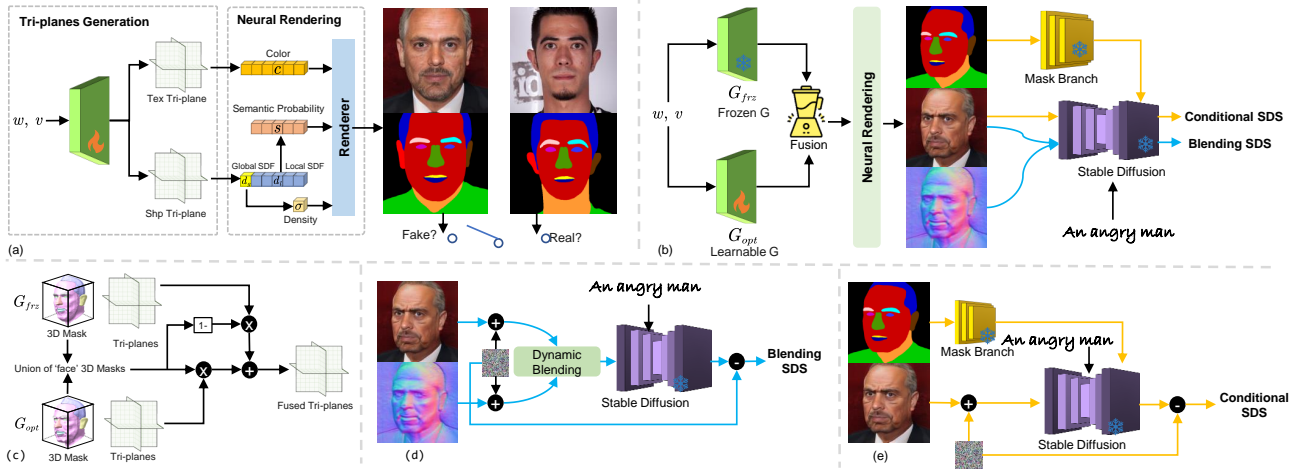


Figure 2. Framework of MaTe3D. MaTe3D Generator (a) consists of Tri-planes Generation and Neural Rendering. Tri-planes Generation constructs 3D volumes of texture and shape in tri-plane representations. Neural Rendering renders 3D-aware image and mask from learned SDF and color. In Inference-optimized editing phase (b), we utilize both a frozen generator (G_{frz}) and a learnable generator (G_{opt}), which were initialized by the generator in (a). We extract 3D masks from both generators to guide feature fusion in tri-planes in (c). In addition, we propose blending SDS (d) and conditional SDS (e) to achieve mask-guided and text-based editing while maintaining consistent texture across multiple views and producing reasonable geometry.

age synthesis, recent methods start to learn 3D-aware models without multi-view supervision. GRAF [34] and piGAN [3] explore NeRF-based 3D-aware synthesis without multi-view supervision pioneeringly. StyleNeRF [9] and CIPS-3D [45] adopt progressively upsampling to synthesize high-quality 3D-aware images. StyleSDF [27] merges NeRF and Signed Distance Function (SDF) [28] which can not only obtain the similar performance as aforementioned methods, but also get smooth 3D complex shape. EG3D [4] introduces a hybrid explicit-implicit 3D representation and produces high-resolution image as well as brings implicitly learned mesh to a new level of meticulousity. The above methods do not consider fine-grained locally-controllable face editing. in the field of mask-guided editing, FENeRF [40] pioneers the 3D-aware face local editing by decoupled latent codes to generate corresponding facial semantics and texture in a spatial aligned 3D volume with shared geometry. IDE-3D [39], the descendant of FENeRF, allows semantic map based image local control in real time. In the field of text-based editing, LENeRF [14] achieves local manipulation via establishing 3D attention map in 3D features.

Diffusion Models. Diffusion models are gaining attention in image synthesis for their ability to produce high-quality and expressive results. GLIDE [26] trains a diffusion model based on text captions encoded into token embeddings via a transformer. DALLE-2 [31] uses CLIP [30] representations and trains a prior to produce CLIP image embeddings from text captions instead of conditioning directly on text embedding. To address the issue of expensive inference in former methods, latent diffusion model (LDM) [33] achieves the diffusion process in the latent space of pre-trained auto-

encoders. Existing diffusion models also derivative many editing approaches, DiffusionCLIP [18] achieve text-guided image manipulation using the pretrained diffusion models and CLIP loss. PTP [11] and null-text [24] invert the image to the noise via DDIM [38] and use attention map control to achieve text-guided exiting. InstructPix2Pix [2] proposes a pipeline that combines large language model knowledge with text-to-image model to edit images from human instructions. ControlNet [44] adds extra conditions to control image generation in Stable Diffusion [33].

3. Methods

Problem setting. Our goal is to perform mask-guided and text-based portrait editing in a single model. We de-couple MaTe3D into two steps. First, we propose a new SDF-based 3D generator. Since performing mask-guided editing mainly happens in local areas, our generator learns both the global and local representations jointly. To learn effectively the global and local representations at the same time, we propose two new objectives: SDF and density consistency losses. When directly manipulating the generator with both mask and text information, the system suffers from two challenges: *3D quality degradation* and *unstable appearance*. To overcome these limitations, in the second step we introduce two techniques based on the Score Distillation Sampling (SDS) [29], including a blending SDS loss and a conditional SDS loss.

Overview. We outline the proposed *MaTe3D* pipeline in Fig. 2, which consists of two main parts: the proposed generator (Fig. 2(a)) and the inference-optimized editing (Fig. 2(b)). In Sec. 3.1, we provide details on the gener-

ator architecture, SDF-based neural rendering and training objectives. During the editing phase (Sec. 3.2), we construct a fused generator by combining a frozen and a learnable generator. This fused generaotor is updated by the proposed blending SDS loss(Fig. 2(c)) and conditional SDS loss (Fig. 2(d)).

3.1. MaTe3D Generator

As shown in Fig. 2(a), our MaTe3D Generator contains two parts: *tri-planes generation* and *neural rendering*. Let v and w be a camera pose and a latent code, respectively.

Tri-planes Generation. As shown in Fig. 2(a), we use a StyleGAN-based generator G to generate both texture tri-plane ($f_{tex-tri}$) and shape tri-plane ($f_{shp-tri}$). This design allows our network to learn physically-plausible geometries and improve image quality. Then we use two separate MLP decoders to learn color features (c) and SDF values (d). In this processing, the learned SDF values include not only the global face d_g , but also specific decompositional facial components such as the nose, eyes, and mouth ($\{d_{l1}, d_{l2}, \dots, d_{ln}\}$). Here, n represents the number of semantic parts.

Neural Rendering. In the proposed generator, we adopt SDF to obtain a watertight and compact 3D facial surface. The regressed values in SDF represent the distances from each coordinate point to the modeled surface. Negative values indicate that the queried points are inside the surface, while positive values indicate that they are outside.

Density feature generation. Inspired by StyleSDF [27] and VolSDF [43], we convert these signed distance values into density values for volume rendering. This conversion is formulated as follows:

$$\sigma_g = K_\alpha(d_g) = \frac{1}{\alpha} \cdot \text{Sigmoid}\left(\frac{-d_g}{\alpha}\right), \quad (1)$$

$$\sigma_{li} = K_\alpha(d_{li}) = \frac{1}{\alpha} \cdot \text{Sigmoid}\left(\frac{-d_{li}}{\alpha}\right), \quad (2)$$

where the σ_g is the density value of the global face and the σ_{li} ($i = 1, \dots, n$) is for local facial components. The learnable hyper-parameter α controls the density value tightness around the surface boundary [27]. It is shared among both global SDF values and the decomposed local SDF values.

Implicit semantic generation. To learn a 3D-aware semantic mask, existing methods [39, 40] typically add an additional head to predict a 3D semantic field. The field was then treated as a color field and used to render a 2D mask. However, our experiments have shown that this design will lead to poor geometries (see Fig. 4). To address this issue, we use the strong association between semantic information and the decompositional geometries. We expect that the semantic class remains consistent within one geometry class, and changes rapidly when crossing the boundary of

different semantic classes. Inspired by the success of scene representation in [42], we directly convert SDF into semantic in generative radiance field:

$$s_i = \frac{\gamma}{1 + \exp(\gamma d_i)}, \quad (3)$$

where the γ is a hyper-parameter to control the smoothness of the function.

Feature map generation. We use a neural renderer to generate the color feature map C_{feat} and low-resolution semantic map S^{thumb} based on the learned density, semantic probabilities, and color features. The first 3 channels of C_{feat} store the low-resolution portrait I^{thumb} . To obtain a high-resolution portrait and semantic mask, we employ a dual StyleGAN-based sampler that synthesizes the high-resolution portrait I^h and semantic mask S^h using the color feature map C_{feat} and low-resolution semantic map S^{thumb} . This sampler is modulated by corresponding latent codes and predicts the residuals of the low-resolution portrait I^{thumb} and low-resolution semantic map S^{thumb} using the shared intermediate color feature map C_{feat} .

Optimization. Naively optimizing a SDF-based generator is hard with the aim to learn simultaneously the global and local representations. Thus, we propose SDF and density consistency losses. These techniques contribute to effectively integrating global and local representations. The full loss function consists of several losses:

Dual Adversarial Loss: We use a dual discriminator to model the distribution of portrait and semantic mask. The discriminator takes concatenation of the portrait image (I^{thumb}, I^h) and semantic mask (S^{thumb}, S^h) as input. We apply classic non-saturating adversarial loss with R1 regularization to obtain \mathcal{L}_{adv} .

SDF Consistent Loss: The SDFs represent the 3D surfaces of objects. To maintain geometrical consistency, we integrate local facial SDFs that should be equivalent to the global SDF. Specifically, by taking the minimum value from a series of decompositional SDFs, we can obtain the combined shape which should align with the global shape. Therefore, we define the signed distance consistent loss as follows:

$$\mathcal{L}_{sdf} = \|d_g, \min(d_{l1}, d_{l2}, \dots, d_{ln})\|^2, \quad (4)$$

Density Consistent Loss: Further, we convert the learned signed distance values to density values and get the following density consistent loss:

$$\mathcal{L}_\sigma = \|\sigma_g, \sum_{i=1}^n \sigma_{li}\|^2, \quad (5)$$

Regularization Loss: We introduce three regularization losses: Eikonal loss (\mathcal{L}_{eik}) to ensure SDFs are physically

valid [27], minimal surface loss (\mathcal{L}_{surf}) to prevent the SDFs from modeling spurious and non-visible surfaces, and density regularization loss (\mathcal{L}_{reg}) to regularize the density convert from SDF to prevent "seam" artifacts.

In summary, the loss of SDF-based generator is:

$$\mathcal{L}_g = \lambda_{adv} \mathcal{L}_{adv} + \lambda_{sdf} \mathcal{L}_{sdf} + \lambda_{\sigma} \mathcal{L}_{\sigma} + \lambda_{eik} \mathcal{L}_{eik} + \lambda_{surf} \mathcal{L}_{surf} + \lambda_{reg} \mathcal{L}_{reg}, \quad (6)$$

where the hyper-parameters λ_{adv} , λ_{sdf} , λ_{σ} , λ_{eik} , λ_{surf} and λ_{reg} balance the contribution of each losses.

3.2. Inference-optimized editing Phase

Our goal is to use a modified semantic mask S^{target} and a text prompt y (e.g., 'a woman wrinkles on face') to edit the content and structure of the input image I . Fig. 2(b) shows the inference-optimized editing phase of MaTe3D. It consists of a frozen generator G_{frz} and a learnable generator G_{opt} . Both G_{frz} and G_{opt} are initialized by the well-trained generator from Sec. 3.1. As shown in Fig. 2(c), we leverage G_{frz} and G_{opt} to extract 3D masks that guide feature fusion in tri-planes from both generators, allowing us to synthesize multi-view output images. For more details about fusion, please refer to **sup. mat.**

When directly manipulating the generator with both mask and text information, the system suffers from two challenges: *3D quality degradation* and *unstable appearance*, see Fig. 8. To overcome these limitations, we introduce two techniques: a blending SDS loss Fig. 2(d) and a conditional SDS loss Fig. 2(e). The former aims to overcome the mismatch problem between texture and geometry, which leads to 3D quality degradation. We compute SDS considering the dynamic blend of image and normal. The conditional SDS loss improves insufficient 3D-aware control, avoiding an unstable appearance.

Blending SDS The original implementation of SDS loss primarily focuses on texture, which causes a mismatch between geometry and appearance, ultimately harming fidelity. To address this issue, we propose to align geometry and appearance by computing SDS on both RGB images I and normal map N . Fig. 2(c) shows the details of blending SDS. Specifically, using a pre-trained SDF-based generator g parameterized with θ , we generate RGB images I and normal maps N , as $(I, N) = g(\theta)$. Given target prompt y , we compute blending SDS as:

$$\nabla_{\theta} \mathcal{L}_{B-SDS} = \mathbb{E}_{\epsilon, t} [w(t)(\epsilon - \epsilon_{\phi}(\hat{z}_t, y, t) \frac{\partial \hat{z}}{\partial N} \frac{\partial N}{\partial \theta} + w(t)(\epsilon - \epsilon_{\phi}(z_t^I, y, t) \frac{\partial z^I}{\partial I} \frac{\partial I}{\partial \theta})], \quad (7)$$

where z_t^I and z_t^N denote the latent representations of RGB image I and normal map n , respectively. $\hat{z} = \mu z^I + (1 - \mu) z^N$ represents a blending latent, where μ is a dynamically

sampled value ranging from 0 to 1. Note the proposed loss differs from TADA [21], which uses a fixed value to fuse texture and geometry.

Conditional SDS. Although blending SDS can provide alignment between appearance and geometry, it still struggles to produce satisfactory results due to unstable texture caused by insufficient 3D-aware control [10]. This leads to ambiguity across different views when applying SDS loss directly to multi-view images. Using 3D-priors could alleviate this issue [10]. However, these 3D-priors (such as 3D-aware target mask) is lacking in our task. To address this issue, we propose a conditional SDS that uses the generated mask m as a conditional for ControlNet, which build a link between the generator and the diffusion prior. As shown in Fig. 2(e). We first train ControlNet (including a mask encoder) conditioning the image and mask pairs. With the well-optimized mask encoder, we can formulate conditional SDS as:

$$\nabla_{\theta} \mathcal{L}_{C-SDS} = \mathbb{E}_{\epsilon, t} [w(t)(\epsilon - \epsilon_{\phi}(z_t^I, y, m, t) \frac{\partial z^I}{\partial I} \frac{\partial I}{\partial \theta})]. \quad (8)$$

Our conditional SDS utilizes an alternating updating scheme to iteratively update the condition of ControlNet and consolidate it into multi-view consistency. This design gradually incorporates diffusion priors conditioned by 3D-aware information into the 3D content. Although the process initially computes an incorrect gradient during optimization, the interaction between front-view supervision and conditional SDS ensures that the results converge to maintain texture consistency and conform to the modified mask.

In summary, we first pretrain our proposed generators on training dataset. Then, we train ControlNet on Stable Diffusion 1.5 with mask condition, utilizing images and annotations. Finally, when editing image, we fix both the generator and ControlNet, update a new well-initialized generator with the proposed blending SDS and conditional SDS.

4. Experiments

Implementation Details The detailed implementation of training our generator and inference-optimized editing can be found in **sup. mat.**

CatMask-HQ The current mask-based editing methods are mainly validated on CelebA-HQ Mask [20] or FFHQ [15], both of which are datasets of human faces. This limits our exploration of model generalization and expansion. Although some few-shot techniques have generated faces and masks in other domains, like cat faces [6], the quality of the image and mask is poor with obvious aliasing. In this paper, we propose CatMask-HQ, a dataset containing approximately 5,060 annotations for cat faces in AFHQ [7]. We have enlisted professional data annotation experts to assist us with labeling. Fig. 3 compares the proposed dataset

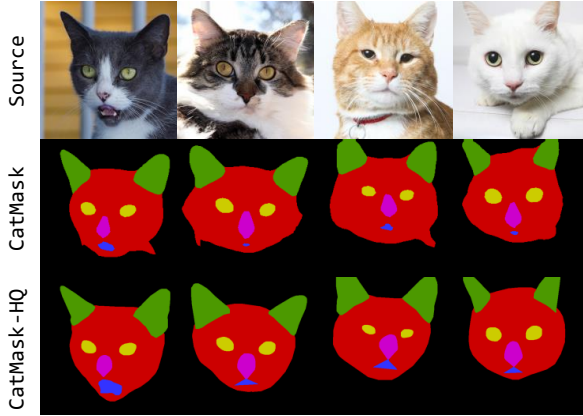


Figure 3. Dataset qualitative comparisons with an existing dataset. CatMask-HQ has superior annotation quality.

with CatMask of Sem2NeRF [6]. For a fair comparison, we label AFHQ using the segmentation model from [6] instead of using sampled cats from pi-GAN [3] to obtain CatMask. For more details, please refer to **sup. mat.**.

Baselines We evaluate the generator of MaTe3D against SOTA generators: FENeRF [40], StyleNeRF [9], StyleSDF [27], EG3D [4] and IDE-3D [39]. We evaluate MaTe3D using two editing methods: text-based and mask-text-hybrid editing. For text-based editing, we compared MaTe3D with LENeRF, FENeRF+StyleCLIP and IDE-3D+StyleCLIP. However, due to the disorganized official code of LENeRF, we reproduced it ourselves for accurate results. We reproduce FENeRF+StyleCLIP and IDE-3D+StyleCLIP for comparison purposes. In hybrid editing, we compare two baselines: FENeRF+StyleCLIP and IDE-3D+StyleCLIP with mask and text acts simultaneously.

4.1. MaTe3D generator Evaluations

We adopt 3 metrics to comprehensively validate the synthesis quality of generated images in quantitative terms. The lower Frechet Inception Distance (FID) [13] and Kernel Inception Distance (KID) [1] indicate higher quality of synthesized images. Multi-view identity consistency (ID) [5] calculates the face similarity across different sampled camera pose. As shown in Tab. 1, MaTe3D achieves comparable results with SOTAs in terms of FID, KID and ID. Visualized results are shown on **sup. mat.**.

In following section we present that MaTe3D is able to learn a well-established geometries, which contributes to accurate mask and provides view consistency results.

Decompositional Geometries: qualitative result. We compare MaTe3D with two other state-of-the-art methods: FENeRF and IDE-3D. As shown in Fig. 4, Mate3D outperforms its predecessors. FENeRF produces visually irritating staircasing artifacts [25] (also known as bulls eye

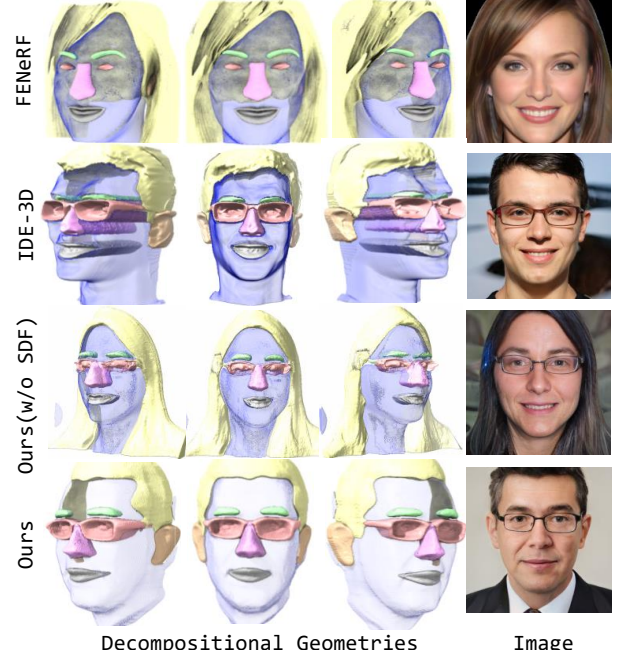


Figure 4. Qualitative comparison with the state-of-the-art methods on decompositional geometries. MaTe3D has more consistent and well-decompositional meshes than FENeRF (staircase artifacts), IDE-3D (inaccurate density distribution along rays) and Ours(w/o SDF, inaccurate eye modeling). We merge some classes for demonstration purposes.

Method	FID \downarrow	KID \downarrow	ID \uparrow
FENeRF [40]	29.0	3.728	0.61
StyleNeRF [9]	7.8	0.220	0.62
StyleSDF [27]	13.1	0.269	0.74
EG3D [4]	4.7	0.132	0.77
IDE-3D [39]	4.6	0.130	0.76
MaTe3D	5.1	0.215	0.79

Table 1. Quantitative comparison with the state-of-the-art methods. The comparison results are quoted from IDE-3D [39].

	Cham. \downarrow	Norm. \uparrow
IDE-3D [39] w nose	3039.3770	0.0443
IDE-3D [39] w nose, mouth	3084.0366	0.0445
IDE-3D [39] w nose, mouth, hair	2607.2324	0.0450
IDE-3D [39] w nose, mouth, hair, ear	2677.9805	0.0451
MaTe3D w nose	1419.5851	0.0934
MaTe3D w nose, mouth	1424.8981	0.0927
MaTe3D w nose, mouth, hair	528.1699	0.0877
MaTe3D w nose, mouth, hair, ear	528.7918	0.0878

Table 2. Evaluation on Chamfer-distance (L1) and normal consistency score (Norm.) [22] between representative editable 3D-aware generative model with MaTe3D.

effect [36]) that are particularly noticeable when viewing small objects up close. We believe this is due to sparse and clustered sampling points in the frustum of FENeRF. IDE-

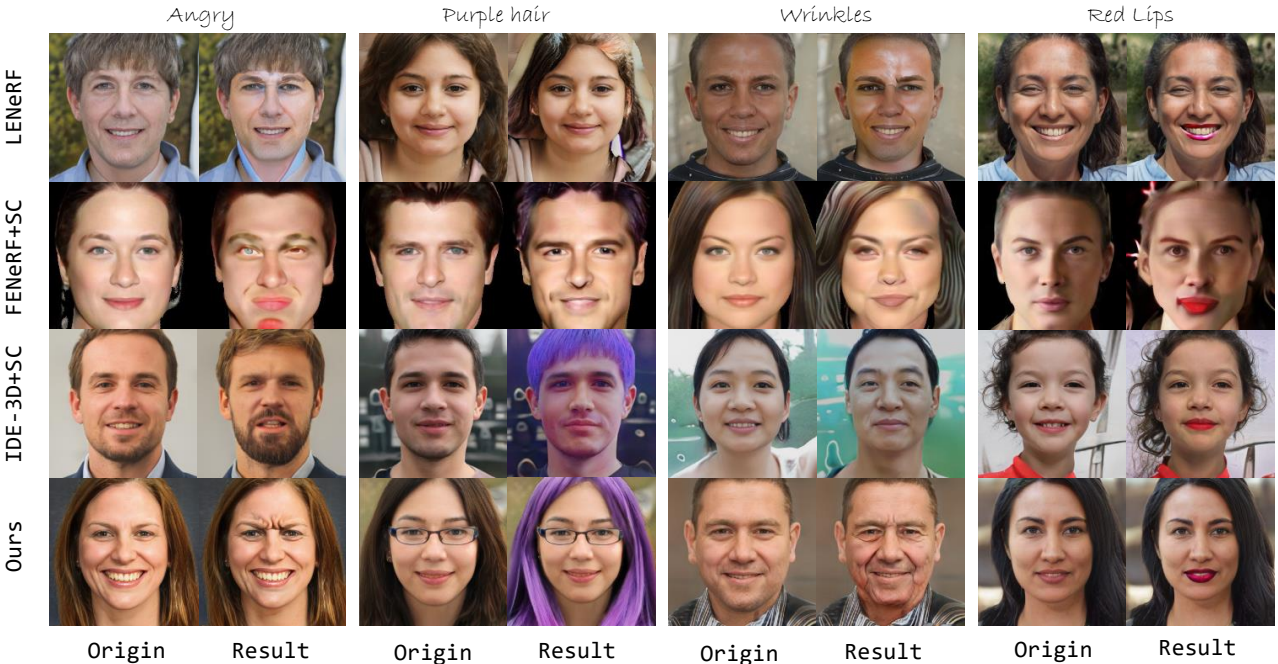


Figure 5. Text-based Editing. Our method can edit images using text while preserving the mask stability, unlike other methods that fail to maintain an unchanged mask or synthesize unimpressive texture. Here, 'SC' represents 'StyleCLIP'.

3D produces photorealistic semantic-aware images of relatively compact whole faces. However, it fails to maintain a well-established 0 level-set in its neural radiance field, resulting in constant density distribution along rays even for local parts like nose, mouth and eyes. This problem may be due to ignore the association between geometries and semantic information, which leads to not-well-disentangled underlying local geometries.

Decompositional Geometries: quantitative result. We aim to investigate the compositional consistency in Mate3D in quantitative way. Our experiments involves combining local facial features with a hollow mesh and comparing it to the original whole face. The results, presented in Tab. 2, demonstrate that MaTe3D significantly enhances 3D surface reconstruction quality compared to IDE-3D. Note that we do not include FENeRF in this comparison as its produced geometries have different resolutions than those of MaTe3D and IDE-3D, making it an unfair comparison. MaTe3D outperforms IDE-3D by large margins in terms of Chamfer-L1 (approximately 1/5 of IDE-3D) and normal consistency (approximately 2 times of IDE-3D), indicating its superior performance in integrity and compositionality.

4.2. Edit Results

Comparison with Text-based Method. In Fig. 5, we show the results of text-based editing. When using CLIP for text-based editing, LENeRF (unofficial reproduction) struggles to produce diverse images, and suf-

fers from insufficient expressive ability and scalability. Although FENeRF+StyleCLIP is able to generate images that match the text, other attributes have been unexpected changed. Additionally the edited images are low quality. IDE-3D+StyleCLIP suffers from a similar issue as FENeRF+StyleCLIP, where the model tends to generate images based on text, which harms the controlled structure of the mask. Our method produces high-quality textures that are faithful to the text prompt and maintain structural stability. We report the CLIPScore [12] value, which measure the correlation between edited images and input texts. We have the best CLIPscore (0.791) comparing with LENeRF (0.612), FENeRF+StyleCLIP (0.729), and IDE-3D+StyleCLIP (0.762). These results further support the subjective superiority of our method.

Comparison with Mask-guided Text-based Method. As shown in Fig. 6, we present qualitative comparisons of our method with existing methods for both mask and text. Our results show high-quality performance in both the mask and text. However, all baselines struggle to effectively utilize both information of mask and text. Some prioritize preserving the mask at the expense of ignoring the text (e.g., FENeRF+StyleCLIP with prompt 'blue sweater'), while others focus solely on matching the text and disregard the mask (e.g., IDE-3D+StyleCLIP with prompt 'christmas hat, Afro hair'). This highlights a lack of balance between the roles of mask and text during synchronous editing within baseline methods.

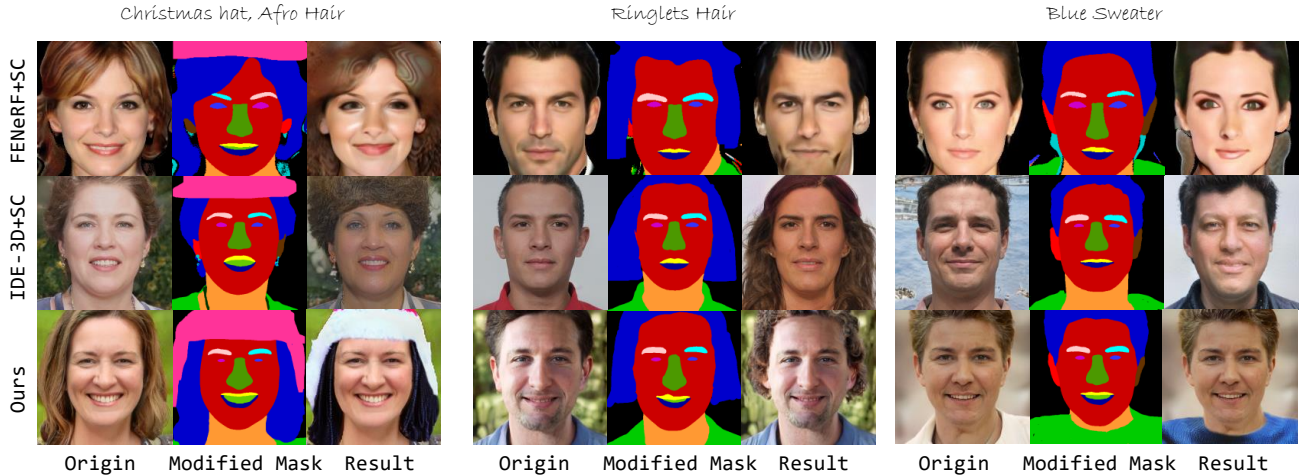


Figure 6. Mask-guided Text-based Editing. Our method allows for synchronous editing of images using both text and mask. The generated images meet the above two conditions simultaneously. Other methods fail to balance the two conditions and produce unreasonable results.

4.3. Ablation Study

Local SDFs Representations We conduct an ablation study on the local SDFs representations. As depicted in Fig. 4, Ours (w/o SDFs) generates photorealistic images and semantic-aware masks, but suffers from unsatisfactory geometries. Benefiting from the design of our generator architecture, the results without SDFs have superior geometries compared to IDE-3D [39], but errors still exist in modeling eyeglasses (incomplete edges) and nose (longer and deeper than normal). These errors occur due to a loss of connection among decompositional facial components. The poor geometry leads to less accurate masks

We randomly sample 1,000 images and masks, then used a pre-trained face segmentation model to predict ground-truth masks. We find that using global and local SDF representations results in a higher mIoU of 0.873, while 'w/o SDF' only reaches 0.812. Our method significantly improves mask accuracy with the support of global and local SDFs and their accompanying geometric constraints. Additionally, we observe that using global and local SDF representations helps maintain view-consistency during the editing phase Fig. 7. Ignoring global and local representations can cause inconsistent results, particularly when adding facial accessories during editing.

Blending SDS and Conditional SDS. As shown in Fig. 8, we conducted an ablation study on our proposed blending SDS and conditional SDS. Our observations indicate that without blending SDS, image synthesis in novel views results in artifacts in image and quality degradation in 3D due to a mismatch between the underlying geometry and appearance (e.g., background and cloth), which further affects mask quality (e.g., aliasing in hair). Without conditional SDS, the editing phase loses 3D-aware control, leading to unstable textures, noticeable blurring, and discontin-

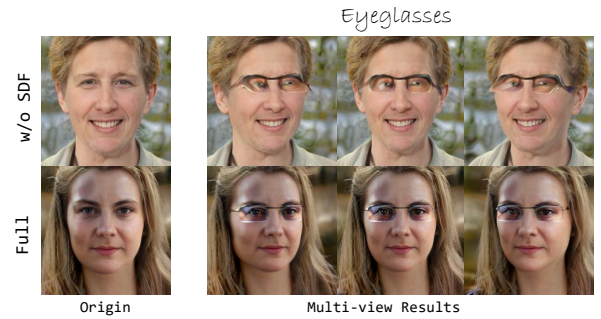


Figure 7. Ablation study of utilizing SDF representations in generator. With SDF, our method produces high-fidelity and view-consistency results.

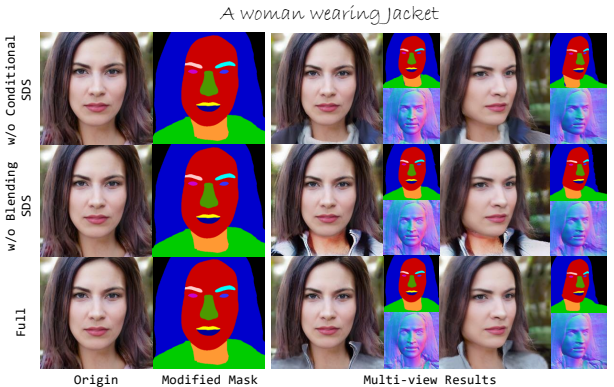


Figure 8. Ablation study of blend SDS and condition SDS. By utilizing blend SDS and condition SDS, we can attain high-quality 2D and 3D results while maintaining consistency between texture and geometry.

uous masks. Additionally, considering the match between texture and geometry or adding extra 3D-aware control can improve image quality, and reduce the number of iterations needed for convergence.

5. Conclusion

We propose MaTe3D, a novel editing pipeline to support mask-guided and text-based 3D-aware portrait editing. Extensive experiments validate our significant performance over the-state-of-the-art methods. The proposed CatMask extends the mask-based editing domain from face to cat face, and serve as a key dataset to verify the feasibility, extensibility, and generalization of the model.

Limitation Our method achieves efficient mask-guided and text-based portrait editing, but the effectiveness is limited by the design of the proposed generator. The generator adopts SDF to prioritize geometries over image quality.

References

- [1] Mikołaj Bińkowski, Danica J Sutherland, Michael Arbel, and Arthur Gretton. Demystifying mmd gans. *arXiv preprint arXiv:1801.01401*, 2018. 6
- [2] Tim Brooks, Aleksander Holynski, and Alexei A Efros. Instructpix2pix: Learning to follow image editing instructions. In *Proceedings of the IEEE/CVF Conference on Computer Vision and Pattern Recognition*, pages 18392–18402, 2023. 3
- [3] Eric R Chan, Marco Monteiro, Petr Kellnhofer, Jiajun Wu, and Gordon Wetzstein. pi-gan: Periodic implicit generative adversarial networks for 3d-aware image synthesis. In *IEEE Conference on Computer Vision and Pattern Recognition*, pages 5799–5809, 2021. 3, 6
- [4] Eric R. Chan, Connor Z. Lin, Matthew A. Chan, Koki Nagano, Boxiao Pan, Shalini De Mello, Orazio Gallo, Leonidas Guibas, Jonathan Tremblay, Sameh Khamis, Tero Karras, and Gordon Wetzstein. Efficient geometry-aware 3D generative adversarial networks. In *IEEE Conference on Computer Vision and Pattern Recognition*, 2022. 2, 3, 6
- [5] Shu-Yu Chen, Feng-Lin Liu, Yu-Kun Lai, Paul L Rosin, Chunpeng Li, Hongbo Fu, and Lin Gao. Deepfaceediting: Deep face generation and editing with disentangled geometry and appearance control. *arXiv preprint arXiv:2105.08935*, 2021. 6
- [6] Yuedong Chen, Qianyi Wu, Chuanxia Zheng, Tat-Jen Cham, and Jianfei Cai. Sem2nerf: Converting single-view semantic masks to neural radiance fields. *arXiv preprint arXiv:2203.10821*, 2022. 5, 6, 3
- [7] Yunjey Choi, Minje Choi, Munyoung Kim, Jung-Woo Ha, Sunghun Kim, and Jaegul Choo. Stargan: Unified generative adversarial networks for multi-domain image-to-image translation. In *CVPR*, pages 8789–8797, 2018. 5
- [8] Ian J. Goodfellow, Jean Pouget-Abadie, Mehdi Mirza, Bing Xu, David Warde-Farley, Sherjil Ozair, Aaron C. Courville, and Yoshua Bengio. Generative adversarial nets. In *Advances in Neural Information Processing Systems*, 2014. 2
- [9] Jitao Gu, Lingjie Liu, Peng Wang, and Christian Theobalt. Stylernerf: A style-based 3d aware generator for high-resolution image synthesis. In *International Conference on Learning Representations*, 2022. 2, 3, 6
- [10] Xiao Han, Yukang Cao, Kai Han, Xiatian Zhu, Jiankang Deng, Yi-Zhe Song, Tao Xiang, and Kwan-Yee K Wong. Headsculpt: Crafting 3d head avatars with text. In *Thirty-seventh Conference on Neural Information Processing Systems*, 2023. 5
- [11] Amir Hertz, Ron Mokady, Jay Tenenbaum, Kfir Aberman, Yael Pritch, and Daniel Cohen-Or. Prompt-to-prompt image editing with cross attention control. *arXiv preprint arXiv:2208.01626*, 2022. 3
- [12] Jack Hessel, Ari Holtzman, Maxwell Forbes, Ronan Le Bras, and Yejin Choi. CLIPScore: a reference-free evaluation metric for image captioning. In *EMNLP*, 2021. 7
- [13] Martin Heusel, Hubert Ramsauer, Thomas Unterthiner, Bernhard Nessler, and Sepp Hochreiter. Gans trained by a two time-scale update rule converge to a local nash equilibrium. *Advances in neural information processing systems*, 30, 2017. 6
- [14] Junha Hyung, Sungwon Hwang, Daejin Kim, Hyunji Lee, and Jaegul Choo. Local 3d editing via 3d distillation of clip knowledge. In *Proceedings of the IEEE/CVF Conference on Computer Vision and Pattern Recognition*, pages 12674–12684, 2023. 2, 3
- [15] Tero Karras, Samuli Laine, and Timo Aila. A style-based generator architecture for generative adversarial networks. In *IEEE Conference on Computer Vision and Pattern Recognition*, pages 4401–4410, 2019. 2, 5, 1
- [16] Tero Karras, Samuli Laine, Miika Aittala, Janne Hellsten, Jaakko Lehtinen, and Timo Aila. Analyzing and improving the image quality of stylegan. In *IEEE Conference on Computer Vision and Pattern Recognition*, pages 8107–8116, 2020.
- [17] Tero Karras, Miika Aittala, Samuli Laine, Erik Häkkinen, Janne Hellsten, Jaakko Lehtinen, and Timo Aila. Alias-free generative adversarial networks. In *Proc. NeurIPS*, 2021. 2
- [18] Gwanghyun Kim, Taesung Kwon, and Jong Chul Ye. Diffusionclip: Text-guided diffusion models for robust image manipulation. In *Proceedings of the IEEE/CVF Conference on Computer Vision and Pattern Recognition*, pages 2426–2435, 2022. 3
- [19] Diederik P. Kingma and Jimmy Ba. Adam: A method for stochastic optimization. In *International Conference on Learning Representations*, 2015. 1
- [20] Cheng-Han Lee, Ziwei Liu, Lingyun Wu, and Ping Luo. Maskgan: Towards diverse and interactive facial image manipulation. In *Proceedings of the IEEE/CVF Conference on Computer Vision and Pattern Recognition*, pages 5549–5558, 2020. 5
- [21] Tingting Liao, Hongwei Yi, Yuliang Xiu, Jiaxiang Tang, Yangyi Huang, Justus Thies, and Michael J Black. Tada! text to animatable digital avatars. *arXiv preprint arXiv:2308.10899*, 2023. 5
- [22] Lars Mescheder, Michael Oechsle, Michael Niemeyer, Sebastian Nowozin, and Andreas Geiger. Occupancy networks: Learning 3d reconstruction in function space. In *Proceedings of the IEEE/CVF conference on computer vision and pattern recognition*, pages 4460–4470, 2019. 6
- [23] Ben Mildenhall, Pratul P Srinivasan, Matthew Tancik, Jonathan T Barron, Ravi Ramamoorthi, and Ren Ng. Nerf:

Representing scenes as neural radiance fields for view synthesis. In *European conference on computer vision*, pages 405–421, 2020. 2

[24] Ron Mokady, Amir Hertz, Kfir Aberman, Yael Pritch, and Daniel Cohen-Or. Null-text inversion for editing real images using guided diffusion models. In *Proceedings of the IEEE/CVF Conference on Computer Vision and Pattern Recognition*, pages 6038–6047, 2023. 3

[25] Mostafa Morsy Abdelkader Morsy, Alan Brunton, and Philipp Urban. Shape dithering for 3d printing. *ACM Trans. Graph.*, 2022. 6

[26] Alex Nichol, Prafulla Dhariwal, Aditya Ramesh, Pranav Shyam, Pamela Mishkin, Bob McGrew, Ilya Sutskever, and Mark Chen. Glide: Towards photorealistic image generation and editing with text-guided diffusion models. *arXiv preprint arXiv:2112.10741*, 2021. 3

[27] Roy Or-El, Xuan Luo, Mengyi Shan, Eli Shechtman, Jeong Joon Park, and Ira Kemelmacher-Shlizerman. StyleSDF: High-Resolution 3D-Consistent Image and Geometry Generation. In *IEEE Conference on Computer Vision and Pattern Recognition*, 2022. 2, 3, 4, 5, 6, 1

[28] Jeong Joon Park, Peter Florence, Julian Straub, Richard Newcombe, and Steven Lovegrove. DeepSDF: Learning continuous signed distance functions for shape representation. In *IEEE Conference on Computer Vision and Pattern Recognition*, pages 165–174, 2019. 3

[29] Ben Poole, Ajay Jain, Jonathan T Barron, and Ben Mildenhall. Dreamfusion: Text-to-3d using 2d diffusion. *arXiv preprint arXiv:2209.14988*, 2022. 2, 3

[30] Alec Radford, Jong Wook Kim, Chris Hallacy, Aditya Ramesh, Gabriel Goh, Sandhini Agarwal, Girish Sastry, Amanda Askell, Pamela Mishkin, Jack Clark, et al. Learning transferable visual models from natural language supervision. In *International Conference on Machine Learning*, pages 8748–8763, 2021. 2, 3

[31] Aditya Ramesh, Prafulla Dhariwal, Alex Nichol, Casey Chu, and Mark Chen. Hierarchical text-conditional image generation with clip latents. *arXiv preprint arXiv:2204.06125*, 1(2):3, 2022. 3

[32] Daniel Roich, Ron Mokady, Amit H Bermano, and Daniel Cohen-Or. Pivotal tuning for latent-based editing of real images. *ACM Transactions on graphics (TOG)*, 42(1):1–13, 2022. 3

[33] Robin Rombach, Andreas Blattmann, Dominik Lorenz, Patrick Esser, and Björn Ommer. High-resolution image synthesis with latent diffusion models. In *Proceedings of the IEEE/CVF conference on computer vision and pattern recognition*, pages 10684–10695, 2022. 2, 3

[34] Katja Schwarz, Yiyi Liao, Michael Niemeyer, and Andreas Geiger. Graf: Generative radiance fields for 3d-aware image synthesis. *Advances in Neural Information Processing Systems*, 33:20154–20166, 2020. 3

[35] Tianchang Shen, Jun Gao, Kangxue Yin, Ming-Yu Liu, and Sanja Fidler. Deep marching tetrahedra: a hybrid representation for high-resolution 3d shape synthesis. *Advances in Neural Information Processing Systems*, 34:6087–6101, 2021. 2

[36] Donald Shepard. A two-dimensional interpolation function for irregularly-spaced data. In *Proceedings of the 1968 23rd ACM national conference*, pages 517–524, 1968. 6

[37] Vincent Sitzmann, Julien Martel, Alexander Bergman, David Lindell, and Gordon Wetzstein. Implicit neural representations with periodic activation functions. *Advances in Neural Information Processing Systems*, 33:7462–7473, 2020. 2

[38] Jiaming Song, Chenlin Meng, and Stefano Ermon. Denoising diffusion implicit models. *arXiv preprint arXiv:2010.02502*, 2020. 3

[39] Jingxiang Sun, Xuan Wang, Yichun Shi, Lizhen Wang, Jue Wang, and Yebin Liu. Ide-3d: Interactive disentangled editing for high-resolution 3d-aware portrait synthesis. *ACM Transactions on Graphics (TOG)*, 41(6):1–10, 2022. 2, 3, 4, 6, 8

[40] Jingxiang Sun, Xuan Wang, Yong Zhang, Xiaoyu Li, Qi Zhang, Yebin Liu, and Jue Wang. Fenerf: Face editing in neural radiance fields. In *Proceedings of the IEEE/CVF Conference on Computer Vision and Pattern Recognition*, pages 7672–7682, 2022. 2, 3, 4, 6

[41] Can Wang, Menglei Chai, Mingming He, Dongdong Chen, and Jing Liao. Clip-nerf: Text-and-image driven manipulation of neural radiance fields. In *Proceedings of the IEEE/CVF Conference on Computer Vision and Pattern Recognition*, pages 3835–3844, 2022. 2

[42] Qianyi Wu, Xian Liu, Yuedong Chen, Kejie Li, Chuanxia Zheng, Jianfei Cai, and Jianmin Zheng. Object-compositional neural implicit surfaces. *arXiv preprint arXiv:2207.09686*, 2022. 4

[43] Lior Yariv, Jiatao Gu, Yoni Kasten, and Yaron Lipman. Volume rendering of neural implicit surfaces. *Advances in Neural Information Processing Systems*, 34:4805–4815, 2021. 4

[44] Lvmin Zhang, Anyi Rao, and Maneesh Agrawala. Adding conditional control to text-to-image diffusion models. In *Proceedings of the IEEE/CVF International Conference on Computer Vision*, pages 3836–3847, 2023. 3, 2

[45] Peng Zhou, Lingxi Xie, Bingbing Ni, and Qi Tian. Cips-3d: A 3d-aware generator of gans based on conditionally-independent pixel synthesis. *arXiv preprint arXiv:2110.09788*, 2021. 2, 3

MaTe3D: Mask-guided Text-based 3D-aware Portrait Editing

Supplementary Material

Abstract

In our supplementary material, we present ethical concerns in Sec. 6 and implementation details in Sec. 7. Network Architectures are listed in Sec. 8. Preliminaries that form the basis of MaTe3D is introduced in Sec. 9. Additional experiments are listed in Sec. 10. The detailed descriptions of proposed CatMask-HQ are listed in Sec. 11. The limitations of MaTe3D are analyzed in Sec. 12. Moreover, a video demo about humans and cats can be seen in the **Supplementary Video**.

6. Ethical Concerns

MaTe3D can reconstruct the representation of a given face and then launch region-wise editing by swapping features with reference images. A series of 3D-consistent images can thus be produced by taking advantage of MaTe3D, which means the great potential to empower areas like artistic creation and industrial design. However, the synthesized images could be wrongly identified by face recognition systems with high probability. Besides, downstream applications like single-view 3D inversion and style mixing could be misused for generating edited imagery of real people. Such misusage put cyberspace in danger inevitably. Overall, the use of this technology needs to be more careful and better regulated.

7. Implementation Details

7.1. Setting of Training Generator

We train our generator on FFHQ [15] and proposed CatMask-HQ. To initialize the model, we adopted sphere initialization from StyleSDF [27]. The training is performed on 4 NVIDIA A100 GPUs (80G) using batch size of 8 for 50,000 steps. We utilized Adam optimizer [19] and set the learning rates for the generator and dual discriminator to 0.0025 and 0.002, respectively. For losses, we assigned values of $\lambda_{adv} = 1$, $\lambda_{sdf} = 0.1$, $\lambda_{\sigma} = 0.001$, $\lambda_{eik} = 0.05$, $\lambda_{surf} = 0.1$, and $\lambda_{reg} = 1$.

7.2. Setting of Editing

During editing phase, we optimize learnable generator 2,000 iterations for each target mask and input text prompt, which would take around 2 hour on a single Tesla A100 GPU (80G). Adam [19] optimizer is utilized with learning rate of $3e - 3$.

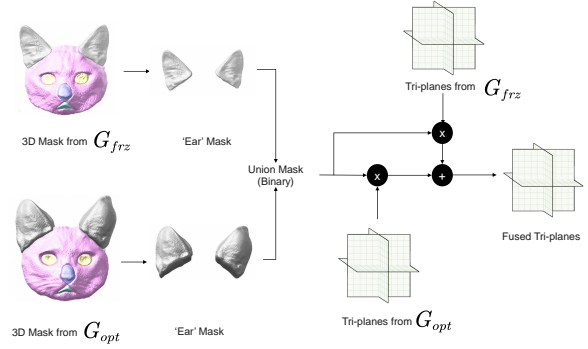


Figure 9. Fusion Pipeline. We combine 3D masks from both generators and unit to create a new 3D mask. This mask guides feature fusion in tri-planes from both generators.

8. Network Architectures

8.1. Fusion Module

Fusion Module can obtain a 3D mask m_{3d} ($BS*3*32*256*256$) directly from regions of edited semantic classes R_i^{frz} from frozen generator and R_i^{opt} from learnable generator, which are established through a strong association of SDFs and semantic information. This is in contrast to existing methods that require learning an additional attention field from sketches to achieve the same result. Here we formulate the Fusion Module as:

$$m_{3d} = \bigcup_{i=1}^n R_i^{frz} \cup \bigcup_{i=1}^n R_i^{opt} \quad (9)$$

$$\hat{f}_{tex} = (1 - m_{3d}) * f_{tex}^{frz} + m_{3d} * f_{tex}^{opt} \quad (10)$$

$$\hat{f}_{shp} = (1 - m_{3d}) * f_{shp}^{frz} + m_{3d} * f_{shp}^{opt} \quad (11)$$

where n denote the number of edited semantic classes, f_{tex}^{frz} ($BS*3*32*256*256$) and f_{shp}^{frz} ($BS*3*32*256*256$) represent the texture and shape tri-planes of the frozen generator G_{frz} . Similarly, f_{tex}^{opt} ($BS*3*32*256*256$) and f_{shp}^{opt} ($BS*3*32*256*256$) represent the texture and shape tri-planes of the learnable generator G_{opt} . By combining these features and get \hat{f}_{tex} and \hat{f}_{shp} , we can generate edited results I_{edit} using neural rendering. The fusion pipeline is shown in Fig. 9.

9. Preliminaries

9.1. Stable Diffusion

Our MaTe3D is highly based on distilling knowledge from Stable Diffusion (SD) which is a type of text-to-image gen-

erative model. SD contains two stage: diffusion process and denoise process. In diffusion process, Gaussian noise would be gradually added to the data with steps of T . In denoise process, a modified UNet would predict noise that should be remove from the sampled Gaussian noise. The optimization process can be formulate:

$$\mathcal{L} = E_{z_0, \epsilon \sim N(0, I), y, t} \|\epsilon - \epsilon_\theta(z_t, y, t)\|^2, \quad (12)$$

where x_0 represents the training data with text condition y , $t \in [0, T]$ represents the timestep, ϵ is the additive Guassian noise and ϵ_θ is the parameters of learnable UNet, $z_t = \alpha_t z_0 + \sigma_t \epsilon$ is the noisy data at timestep of t , α_t and σ_t are predefined functions and related to timestep t .

9.2. ControlNet

ControlNet [44] is an innovative approach that enhances Stable Diffusion by incorporating additional conditions, allowing for the synthesis of images based on input conditions, such as canny edge and pose map. In our implementation of ControlNet, we train it using a n-channel one-hot mask instead of a colorful semantic map as used in the original ControlNet. This mask representation not only supports interactive editing but also enables inpainting pipeline. To achieve this, we employ a mask encoder to map the input mask to the same dimension as the latent code in Stable Diffusion. Additionally, we use zero convolution during training to prevent harmful noise. The optimization process can be formulated as follows:

$$\mathcal{L} = E_{\epsilon \sim N(0, I), t} \|\epsilon - \epsilon_\theta(z_t, y, m_{2d}, t)\|^2, \quad (13)$$

where z_0 represents the latent feature map encoded from training data. The variables y and m_{2d} represent the text condition and mask condition, respectively. The variable $t \in [0, T]$ represents the timestep. Additionally, ϵ is an additive Gaussian noise term and ϵ_θ represents the parameters of a learnable mask encoder. The noisy data at timestep t , denoted as z_t , is given by the equation: $z_t = \alpha_t z_0 + \sigma_t \epsilon$, where α_t and σ_t are predefined functions that depend on the timestep t .

9.3. Score Distillaton Sampling (SDS)

Score Distillation Sampling (SDS) is a technique developed by DreamFusion [29] to distill knowledge from a pre-trained diffusion model into a differentiable 3D representation generator, such as NeRF [23] or DMTet [35]. The 3D representation generator g is parameterized by $\theta \in \Theta$, where Θ is the space of θ with the Euclidean metric. Given the specified camera c , we can obtain the rendered image I using the equation $I = g(\theta, c)$. Then, a random noise would be added to z encoded from image I and the diffusion model is adopt to predict the added noise ϵ from the noisy image with a pre-trained denoising function ϵ_ϕ , given

Method	FID \downarrow	KID \downarrow
StyleNeRF [9]	14.9	0.368
StyleSDF [27]	12.8	0.455
EG3D [4]	2.7	0.041
MaTe3D	2.5	0.078

Table 3. Quantitative comparison with the state-of-the-art methods in cat face.

the noisy image z_t , text embedding y and noise timestep t . The SDS provides gradient to update the generator which parameterized by θ , this can be formulated as:

Score Distillation Sampling (SDS) is a technique introduced by DreamFusion [29] and extensively employed to distill knowledge from a pre-trained diffusion model [33] into a differentiable 3D representation generator (e.g., NeRF [23] or DMTet [35]). Consider a 3D representation generator g is parameterized by θ , given a sampled camera view π , we can obtain the rendered image x by $x = g(\theta)$.

$$\nabla_\theta \mathcal{L}_{SDS}(\phi, \theta) = \mathbb{E}_{\epsilon, t} [w(t)(\epsilon - \epsilon_\phi(z_t, y, t)) \frac{\partial z}{\partial I} \frac{\partial I}{\partial \theta}], \quad (14)$$

where $\epsilon \sim \mathcal{N}(0, I)$, $t \sim \mathcal{U}(0.02, 0.98)$.

10. Additional Experiments

10.1. Visualized Evaluations of Generator

Fig. 10 presents a qualitative comparison of MaTe3D against 3D-aware GANs. It is evident that MaTe3D achieves comparable image quality and better view consistency than the baselines, benefit from the utilization of global and local SDF representations in the generator.

10.2. Results on FFHQ

In Fig. 11 and Fig. 12, we present additional results on text-based editing and mask-guided text-based editing. Our method enables fine-grained manipulation with reasonable textures while preserving geometries to maintain view consistency.

10.3. Results on CatMask-HQ

We present additional results for CatMask-HQ and compare its image quality with EG3D [4], as depicted in Fig. 13 and Tab. 3. Our method produces comparable image quality with better view consistency.

We provide more editing results in Fig. 14. Our method can synthesize stable and anti-aliasing textures, as well as maintain view consistency by synthesizing anti-degradation geometries.



Figure 10. Qualitative comparison in image quality. MaTe3D achieves comparable image quality and better view consistency.

11. CatMask-HQ

We introduce CatMask-HQ, a new mask dataset on cat faces in AFHQ. This dataset includes single view cat face and mask annotations for six classes: background, skin, ears, eyes, nose and mouth. Unlike the CatMask in Sem2NeRF [6], which contains generated images from piGAN [3] and adopts a segmentation network in few-shot learning to obtain pseudo labels, we invite 50 annotators to label our dataset and each annotation would be checked 3 times for accuracy. To ensure fair comparison with previous work, we adopt the same segmentation network as CatMask to label AFHQ and get CatMask. Qualitative comparisons between the pseudo labels and annotated results are shown in Fig. 15. Our proposed dataset has more accurate annotations without any aliasing edges or hollow classes present

in the pseudo labels.

12. Limitations

As previously mentioned, MaTe3D has a natural ability to enable mask-guided text-based editing and has surpassed its baselines. However, there are still some challenging cases that need to be addressed: 1) the image quality may slightly deteriorate when learning better geometry with global and local geometries through SDFs, and 2) the results for real images are not entirely satisfactory. We observe that using the traditional tuning strategy PTI [32] can negatively impact the geometries of SDFs.

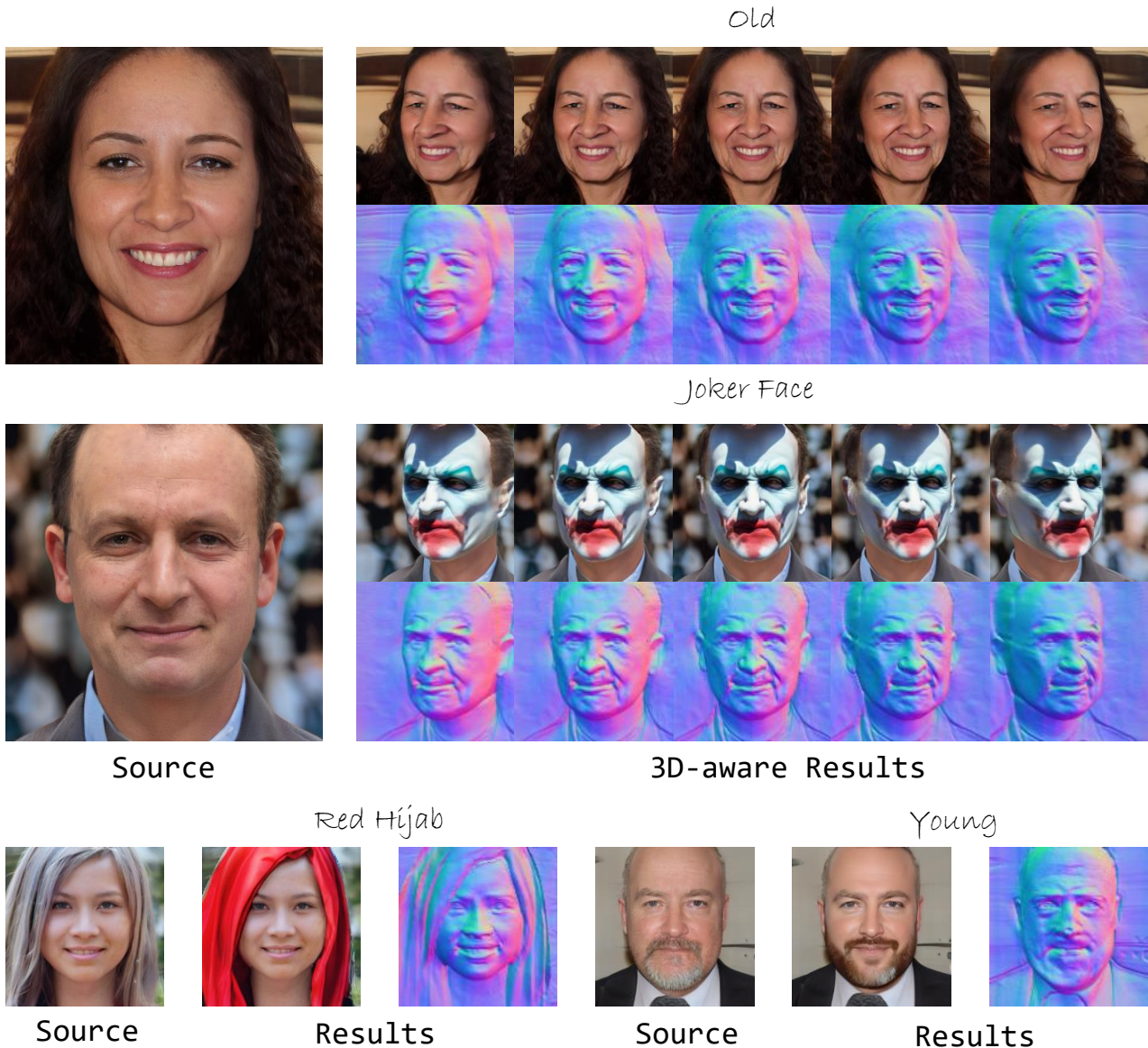


Figure 11. Text-based editing.

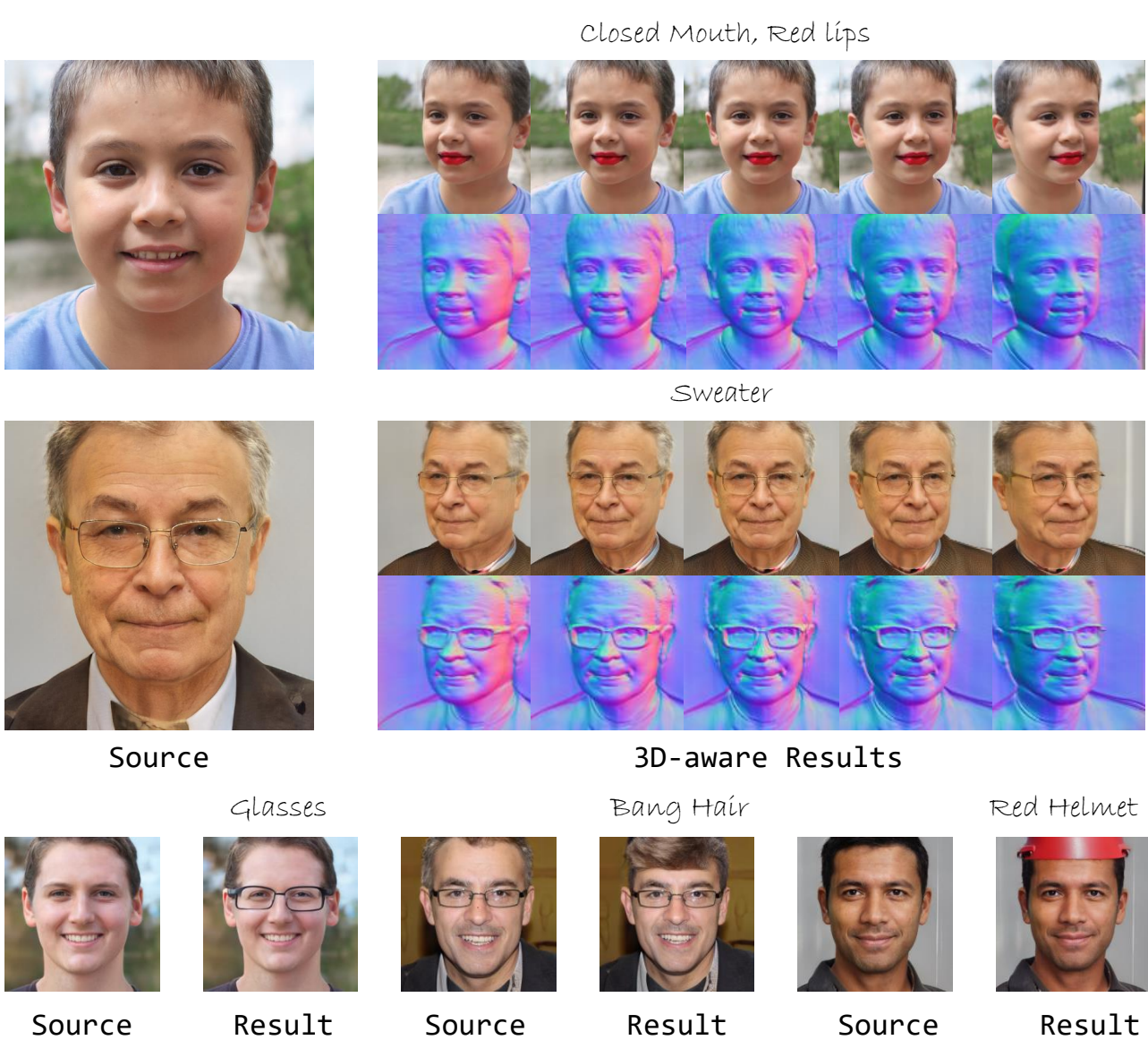


Figure 12. Mask-guided text-based editing.



Figure 13. Qualitative comparision in image quality in cat face. MaTe3D produces images of similar quality and provides improved view consistency.



Fleshy nose



Tiger Face



Big Ears

Source

3D-aware Results

Figure 14. Text-based editing (Fleshy nose and Tiger Face). Mask-guided text-based editing (Big Ears).



Figure 15. Dataset qualitative comparisions with existing methods. CatMask-HQ has superior annotations against baselines.